https://doi.org/10.48047/AFJBS.6.10.2024.7258-7274

Comparison of Hydrophilic and Hydrophobic polymers based matrix Transdermal Patches using Amomum leaf oil as a penetration enhancer

Sudip Das[1*], Bapi Ray Sarkar[2], Koushik Sen Gupta[3]

[1] Department of Pharmaceutics, Himalayan Pharmacy Institute. Majhitar. Rangpo, East Sikkim, India, Pin: 737136.

[2,3] Department of Pharmaceutical Technology, University of North Bengal. India, Pin: 734013

***Corresponding author details:** Bapi Ray Sarkar. Department of Pharmaceutical Technology, University of North Bengal. India, Pin: 734013

Email: brspublication@gmail.com

Article History
Volume 6 issue 10, 2024
Received: 15 May 2024
Accepted: 15 June 2024
doi:
10.48047/AFJBS.6.10.2024.7258-7274

Abstract:

The research manuscript's objective is to develop transdermal patch formulations of Diclofenac potassium utilizing different ratios of Eudragit L-100D (hydrophobic) and Pluronic F-127(hydrophilic) polymers and *Amomum subulatum* leaf oil as a 'penetration enhancer'. In this study, several physical parameters, including moisture content, moisture uptake, tensile strength, flatness, folding endurance, uniformity, weight variation, and thickness were assessed. Formulations were prepared by the solvent evaporation technique after an interaction study between polymers and penetration enhancers. Additionally, the transdermal patches were studied for physicochemical parameters involving permeation studies, mechanical properties, and toxicity studies of skin irritation. Formulations exhibited favourable pre-formulations and post-formulary characteristics. *'In vitro* permeation' was conducted using an USP type-7 dissolution apparatus. The patches demonstrated an apparent absence of potentially harmful skin irritation. Experimental results indicated a controlled and sustained administration of the medicament from the formulation with an increasing proportion of hydrophilic polymer and permeation enhancers with reduced toxicity. The study concludes that Diclofenac potassium can be effectively developed into transdermal patches using *Amomum subulatum* leaf oil as a penetration enhancer for enhanced permeation and sustained drug administration.

Keywords: Pluronic, *Amomum subulatum*, Transdermal drug delivery, Enhanced penetration, USP 7 Dissolution test apparatus.

Introduction

Diclofenac potassium is taken to treat various ailments, including headaches, tooth pain, menstrual cramps, and muscle aches. It also reduces mild-to-moderate inflammation [1]. Some

of these drug brands may also lessen arthritis-related joint stiffness, edema, and discomfort. A non-steroidal anti-inflammatory medication (NSAID) is diclofenac potassium. Its function is to prevent our body from producing some natural inflammatory molecules [2].

Diclofenac potassium exhibits diverse physiochemical attributes, including low water solubility, a modest molecular mass, and a favourable melting point, implying potential skin permeability. Developing a transdermal drug delivery formulation for this medication could potentially alleviate its hepatic system-related adverse effects and maintain a consistent blood level over an extended duration [3]. Common 'side-effects' of Diclofenac potassium, such as upset stomach, diarrhoea, nausea, constipation, and gas, could be addressed through the using 'transdermal patch' [4].

The term "transdermal drug delivery system," or TDDS, refers to a unique dosage form that is applied to the upper epidermal layers of humans. It enters the medication into the bloodstream in a controlled manner, bypassing the first-pass possessions. In comparison to traditional delivery methods like injections or oral administration, this system provides a valuable alternative [5]. By circumventing first-pass metabolism, it enhances the 'therapeutic effectiveness' of pharmaceutical actives, ensures 'controlled release', improves absorption, and promotes better patient compliance [6].

The current investigation utilizes a natural penetration enhancer, specifically *Amomum subulatum* leaf oil. This oil is derived from the *Amomum subulatum* plant of the Zingiberaceae family. Gas chromatography (GC) and gas chromatography-mass spectrometry (GC-MS) analyses reveal the existence of 39 constituents in the oil. Notably, terpinene-4-ol (29.87%), eucalyptol (18.69%), β-phellandrene (7.97%), γ-terpinene (6.67%), and p-cymene (6.20%) are identified as significant components. Oxygenated monoterpenes dominate the essential oil of the plant, constituting 59.03% of the overall oil content.

The matrix-type film (Diclofenac potassium) incorporates a natural permeation enhancer for effective pain treatment. The goal was to facilitate 'controlled drug release' across intact skin. Formulations were refined using a 3^2 full factorial design [7,8]. The patches underwent assessment for a range of factors, such as diffusion studies, folding endurance, drug content, and others.

Examination of Drug- Polymer Physicochemical Compatibility:

FTIR

An FT-IR spectroscopic analysis was done Diclofenac potassium both individually and paired with Eudragit L-100D, Pluronic F127, and Amomum oil [9].

Estimation of 'Essential Oil' by Clevenger Apparatus

Determination of 'volatile oil' content in oil-bearing material employs the Clevenger instrument. Begin by introducing a measured quantity of the leaf into a sample flask, followed by filling the flask with water, maintaining a material-to-water ratio typically at 1:8. Connect the flask to the Clevenger apparatus and initiate water flow into the condenser by turning on the water tap [10]. Activate the heating process using a heating mantle, carefully regulating the heat to allow water-containing oil vapours to enter the receiving tube for graded distillate, while any excess water returns to the flask. Allow the process to continue for eight hours, and subsequently, use a desiccator to cool the assembly, removing any remaining water. Finally, cool the assembly again, ensuring the removal of any water from the distillate receiving tube [11].

Preparation of Transdermal Films

Transdermal film incorporating 'Diclofenac potassium' was formulated using the solvent evaporation system within cylindrical moulds which are made up of glass having open sides

[12]. Backing membrane was prepared by adding a 4% (m/v) polyvinyl alcohol (PVA) solution and drying at room temperature [3,13]. For the drug reservoir, Eudragit L 100D (EU100) and Pluronic F-127 (PL) were dissolved in ethanol. Amomum leaf oil served as a penetration enhancer, and Glycerine (15% w/w of dry polymer weight) functioned as a plasticizer. 'Diclofenac potassium' 50 mg (in 5 ml of ethanol), was introduced into the homogeneous dispersion under slow stirring with a magnetic stirrer. The resulting uniform dispersion was then added onto a PVA backing membrane. After that the formulations were dried at room temperature (refer to Table No. 1. The final formulations were subsequently stored in an airtight zipper pack in a desiccator [14].

Table 1: Different formulation chart

Formulation Code	EU	PL	Penetration enhancer	Plasticizer (% w/w)	Ethanol (ml)	Drug (mg)
F1	250	444	3	30	10	50
F2	56	250	3	30	10	50
F3	56	56	4.5	30	10	50
F4	250	250	4.5	30	10	50
F5	56	444	4.5	30	10	50
F6	444	250	6	30	10	50
F7	250	56	3	30	10	50
F8	250	444	6	30	10	50
F9	444	250	3	30	10	50
F10	444	56	4.5	30	10	50
F11	56	250	6	30	10	50
F12	250	250	4.5	30	10	50
F13	250	56	6	30	10	50
F14	250	250	4.5	30	10	50
F15	444	444	4.5	30	10	50

Evaluation of formulations:

Thickness of Formulations:

Measurements of 'thickness of patches 'were conducted employing a micrometres instrument from Mitutoyo Co., Japan. Four distinct regions on the formed patches were assessed for their thickness using the micrometre, and the resulting average thickness was calculated [12,15].

Folding Endurance:

A patch of specific dimensions (2 cm x 2 cm) was cut and subjected to repeat folding at the same point until it reached the point of rupture [16]. The number of times the film could be folded at the same spot without breaking was used to calculate the value [17].

Drug Content

The formulation was solubilised in a 7.4 pH buffer solution and allowed to stand for 24 hr. in volumetric flask (100 ml) [18]. After 'filtration', The substance that was filtered out, taken drug content was assessed by measuring it using a UV spectrophotometer at 276 nm [9,19].

Flatness study

Three numbers of longitudinal strips were extracted from the each formulation one from the middle and both sides of the formulations [20]. After the measurement of every stripes length the change in length due to flatness non-uniformity was calculated using percent constriction formula. In this formula, 0% constriction corresponds to 100% flatness [21]

Tensile strength:

Tensile strength represents the optimum stress a film can endure before breaking, while elongation gauges a patch's capacity to deform before reaching failure [22]. The patches' tensile strength and percentage elongation were evaluated using tensile strength testing equipment. Rectangular patches measuring 25.4mm x 50mm were securely held between the instrument's jaws. Alteration in strip length under incremental stress was recorded as the load on the strip was gradually elevated to a maximum at a speed of 50mm/min [23] 'Tensile strength' and 'percentage elongation' were measured for three formulations from every batch [17,24].

Percentage Moisture Content:

Each film was individually weighed and kept inside the desiccators had activated silica for 24 hours at ambient temperature. The formulated weighed films were used. 'Until a constant' weight was achieved [25]. The 'percentage moisture content' can be determined using the given formula [26].

Percent moisture content=

Initial weight- final weight/ final weight × 100

Percent Moisture uptake:

These tests were conducted on the formulated films by placing patches inside the desiccator containing a 'saturated potassium chloride solution', exposing them to 84% relative humidity at 'room temperature' until a stable weight was attained [27]. Subsequently, the film were weighed, and the following formula was used on determine the 'percentage moisture uptake' [28].

Percentage moisture uptake=

Final wt – initial wt/ initial wt×100

Water vapour transmission (WVTR):

The WVTR quantifies the quantity of moisture passing through a given area of film during a defined time period [29]. Glass cells were filled with two grams of anhydrous calcium chloride, and the cell rim was covered with a film of known specific area [30]. The assembly was measured accurately and maintained at a 'specific temperature' of 27 ± 2 °C for 24 hr. within a humidity chamber set at a relative humidity (RH) of 80 ± 5% [31].

***In-vitro* skin permeation studies**

***'In-vitro* drug release' studies using reciprocating USP 7 Apparatus:**

The *in vitro* 'drug release' was conducted using a USP-7 dissolution apparatus, following established protocols with certain modifications. A vessel with a volume capacity of 300 ml was attached to the reciprocating apparatus. The internal temperature was upheld at 37.0 ± 0.3 °C, facilitated by a built-in heater for temperature control. The reciprocating discs featured a 2.5 cm stroke depth, and a dipping rate of 45 dips / minute was set. Seven patches were used in each test. The experiment began by placing the vessel inside a water bath filled with 7.4 phosphate buffer solution. Formulations were positioned on the outermost layer of the membrane utilised for dialysis, aligning both on the open side of the reciprocating cylinder [32.33, 34]. The cap was securely closed to ensure proper positioning, and the cylinder was affixed to the agitator rod.[35]

Upon initiating the dissolution apparatus, the reciprocating cylinder descended into the vessel containing 7.4 phosphate buffer solutions, bringing the 'dialysis membrane' into contact with the solution. This allowed the medicament from patch to release the drug getting into the buffer solution via the membrane [36].

Skin Irritation Study:

The study followed OECD Guidelines (ethical number HPI/2021/60/IACE/PP-0190) 404 for acute 'dermal irritation', employing a positive control group exposed to a 0.8% w/v formaldehyde solution, a control group with a placebo patch, and a treated group with Diclofenac potassium-loaded transdermal patches. Diclofenac potassium, mixed with oil, formed a paste for dermal application (2 mg/kg), applied to a 5 cm × 5 cm area of unclipped rabbit trunk. A 2.5 cm × 2.5 cm gauze patch covered the test part, secured with occlusive dressing, and rabbits wore Elizabethan collars. After 4 hours, the patches were taken off, and residual material washed away before scoring dermal reactions, which were absent at 3 min, 1 h, and 4 h post-removal. Confirmatory tests on two more rabbits corroborated initial findings due to their lack of dermal reactions. Additionally, three recurring skin applications over 7 days were conducted.

At the test sites, erythema and oedema were measured. at 1 hour, 24 hours, 48 hours, and 72 hours post-exposure to Diclofenac, both in single and repeated dermal studies on rabbits. Scoring followed OECD guideline [7], using a scale from 0 to 4, where 0 indicated no effect, indicated 4 severe symptoms. The sum of scores for dermal response at each time point resulting from patch removal was divided by three to calculate the mean irritation score per time point for each animal. These scores were then compared to those of control animals receiving distilled water. The primary irritation index was obtained by summing and averaging the mean scores [37].

Result:

Table 2 Results of Formulated patches

Batch code	FE	WV	TS	WVT	MC	MU	UT	% Ft	DC
F_1	79±1.32	0.22	219.35 ±0.02	1.75624×10^{-4} ±0.02	4.25 ± 0.002	6.64 ± 0.001	110± 1.2	99.5±0.003	97.7
F_2	80±1.09	0.21	236.37 ±0.02	1.63121×10^{-4} ±0.03	4.59 ± 0.003	5.70± 0.001	111± 1.2	99.7±0.002	99.3
F_3	79±1.32	0.21	226.44 ±0.01	1.21259×10^{-4} ±0.02	4.39 ± 0.002	2.94 ± 0.001	114± 1.3	99.5±0.003	98.7
F_4	79±1.31	0.21	224.93 ±0.02	1.53121×10^{-4} ±0.04	4.36 ± 0.002	5.92 ± 0.002	110± 0.8	99.3±0.005	98.2
F_5	89±1.31	0.22	208.32 ±0.01	1.96157×10^{-4} ±0.04	4.05 ± 0.002	6.12 ± 0.002	110± 1.4	99.3±0.003	97.10
F_6	93±1.13	0.22	251.07 ±0.02	1.20012×10^{-4} ±0.02	4.87± 0.002	5.81± 0.001	114± 1.3	99.1±0.002	98.3
F_7	86±1.02	0.21	239.14 ±0.01	1.20234×10^{-4} ±0.03	4.64 ± 0.003	2.91 ± 0.003	110± 1.3	99.9±0.003	98.13
F_8	79±1.40	0.21	219.31 ±0.02	1.91012×10^{-2} ±0.02	4.25 ± 0.002	6.64± 0.002	110± 1.2	99.6±0.005	98.94
F_9	91±1.31	0.21	248.43 ±0.03	1.86693×10^{-4} ±0.02	4.82 ± 0.001	3.11 ± 0.002	110± 0.1	99.8±0.003	97.34

F_{10}	91±1.09	0.21	251.14 ±0.03	1.16029×10^{-4} ±0.02	4.88± 0.001	2.64 ± 0.002	108± 0.9	99.2±0.006	99.27
F_{11}	80±1.05	0.21	223.94 ±0.02	1.69132×10^{-4} ±0.02	4.34± 0.002	4.12± 0.001	102± 0.9	99.2±0.006	99.52
F_{12}	79±1.32	0.21	223.94 ±0.02	1.53122×10^{-4} ±0.02	4.34± 0.002	5.91± 0.002	109± 0.9	99.2±0.006	98.66
F_{13}	86±1.02	0.21	241.12 ±0.01	1.20312×10^{-4} ±0.02	4.68± 0.002	2.90± 0.002	110± 0.9	99.0±0.006	99.02
F_{14}	79±1.32	0.21	223.94 ±0.02	1.53119×10^{-4} ±0.02	4.34± 0.002	5.92± 0.001	109± 0.9	99.2±0.006	99.48
F_{15}	95±1.02	0.21	228.37 ±0.01	1.65628×10^{-4} ±0.02	4.43± 0.002	6.51± 0.002	109± 0.9	99.1±0.006	98.08

FE – Folding endurance, WV – weight variation, TS – Tensile strength, WVT – Water vapor transmission, MC – moisture content, MU – Moisture uptake, UT – Uniformity thickness, Ft – Flatness, DC – Drug content

Value represent mean±SD (n=3)

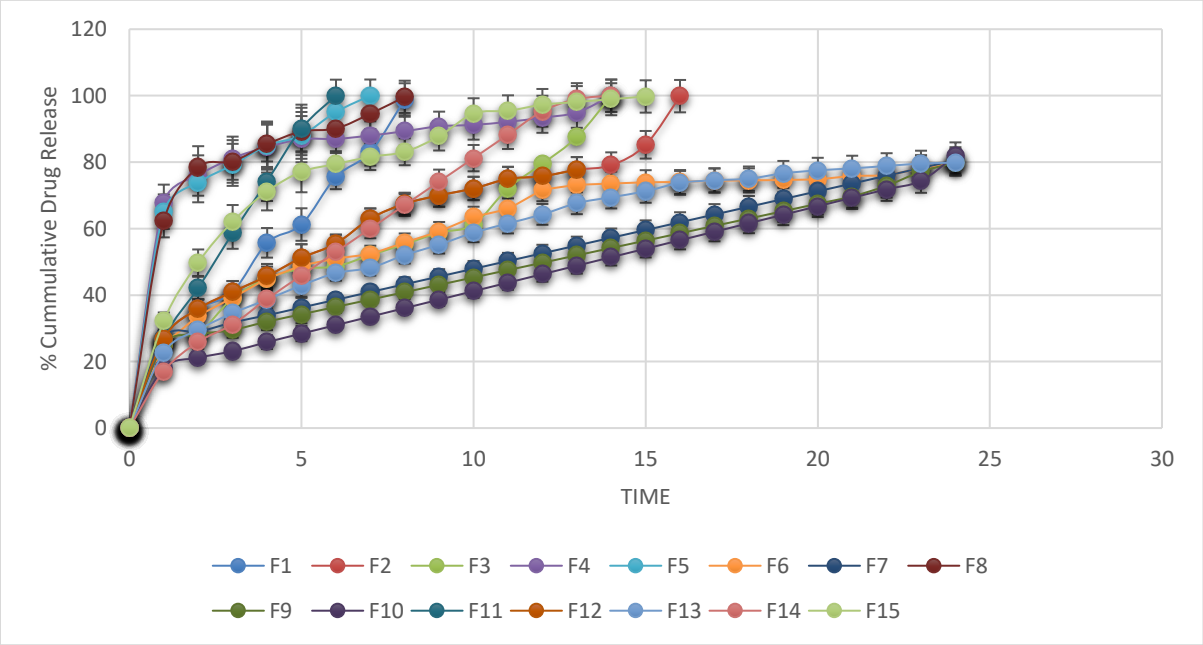

Figure 1: Drug release

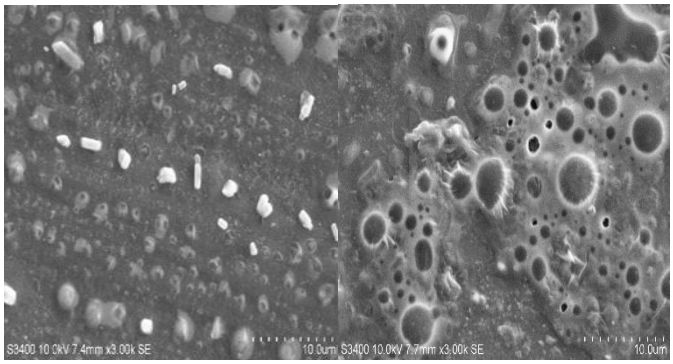

Figure 2: SEM photography of transdermal patch before the study and after the study.

(a) (b) (c)

Figure 3: (a) Before applying the patch, (b) Applying the patch, (c) After applying the patch

The 'folding endurance' experiment was conducted through manual measurements, where films shown the capacity to withstand folding without cracking for 79 to 93 folds before being considered complete. All patches exhibited excellent flexibility and strength (refer to Table 2). The weight variation of each patch's area was meticulously separated into multiple pieces and weighed using a digital balance. Values were felled within the permissible range, ranging from 0.21g to 0.22g, ensuring uniformity in weight and repeatability of the method [37].This uniformity is crucial for consistent drug distribution (Table No 2).

The 'tensile strength' of the formulation ranged from 219.25 gm/cm^2 to 251.07 gm/cm^2. Notably, an elevation in the hydrophilic polymers (PL) concentration correlated with a gradual decrease in the patches' tensile strength. Regarding water vapour transmission, patches made with EU100 exhibited transmissions ranging from 1.20012 x 10-^{4} to 1.69132 x 10-^{4}, indicating permeability to water. Addition of hydrophilic polymer led to an increase in 'water vapour transmission', with TEP10 showing the lowest transmission, likely due to absence of hydrophilic polymer [38,39].

According to Table 2, patches with varying amounts of EU100 -PL displayed a present moisture content ranging from 4.05 to 4.88% w/w. The results specify that an elevation in the levels hydrophilic polymer led to higher 'moisture content'. F10, with highest EU100 concentration, exhibited low moisture content, contributing to material stability and preventing complete drying and brittleness. The 'percentage moisture uptake' ranged from 2.64 to 6.64% for patches with various EU100 and PL proportions (refer to Table 2). F5 showed the maximum moisture uptake, while F10 exhibited the reverse trend. This reduced moisture uptake simultaneously safeguards the patches from 'microbiological contamination' and bulkiness [40].

The uniformity of thickness study, utilizing micrometers with a least count of 0.01mm, revealed that films maintained more than 99% flatness. This characteristic ensures a flat skin application surface, allowing for closer contact and improved medication penetration. 'Drug content' study indicates, the over 97% of the medicament, present in prepared patches, with the drug concentration in various formulations ranging from 97.00 to 99.2%. All formulations met the criteria for adequate drug content.

Drug release data from the *in-vitro* permeation study were applied to different kinetic models, such as 'Zero order', 'first order', and the 'Higuchi model' and 'Korsemeyer-Peppas' release kinetics. A comparative analysis of 'cumulative % drug release' per cm^2 vs. the square root of time profile was plotted for patches composed of EU100 -PL. The Log ARA was calculated to express the First order kinetics. The Korsemeyer-Peppas model, which depicts the diffusion 'kinetics of drug release', was graphed by plotting Log Mt/M∞ against Log time for EU100 -PL. A low n value indicated diffusion-controlled release. The 'coefficient of regression' values for all kinetic models, incorporating *in-vitro* permeation results, showed a burst release for all patch formulations in the drug release study [41].

Response 1: Tensile Strength

Source	**Sum of Squares**	**df**	**Mean Square**	**F-value**	**p-value**	
Model	2268.84	9	252.09	58.46	0.0002	significant
A-EC	870.28	1	870.28	201.81	< 0.0001	
B-PL	842.35	1	842.35	195.33	< 0.0001	
C-PE	7.51	1	7.51	1.74	0.2442	
AB	6.63	1	6.63	1.54	0.2700	
AC	56.78	1	56.78	13.17	0.0151	
BC	0.9216	1	0.9216	0.2137	0.6633	
A^2	198.65	1	198.65	46.07	0.0011	
B^2	31.32	1	31.32	7.26	0.0430	
C^2	257.28	1	257.28	59.66	0.0006	
Residual	21.56	5	4.31			
Lack of Fit	20.91	3	6.97	21.33	0.0451	significant
Pure Error	0.6534	2	0.3267			
Cor Total	2290.40	14				

Factor coding is coded.
Sum of squares is Type III – Partial
Fit Statistics

ANOVA for Linear model

Response 2: Moisture content

Source	**Sum of Squares**	**df**	**Mean Square**	**F-value**	**p-value**	

Model	0.6513	3	0.2171	10.82	0.0013	**significant**
A-EU100	0.3281	1	0.3281	16.35	0.0019	
B-PL	0.3200	1	0.3200	15.95	0.0021	
C-PE	0.0032	1	0.0032	0.1595	0.6973	
Residual	0.2207	11	0.0201			
Lack of Fit	0.2205	9	0.0245	183.71	0.0054	**Not significant**
Pure Error	0.0003	2	0.0001			
Cor Total	0.8720	14				

Factor coding is **coded**.

Sum of squares is **Type III – Partial**

The F-value of the model 10.82 signifies the model's significance. The likelihood a huge F-value occurring solely because of noise is merely 0.13%. Model terms are deemed remarkable when all the P is below 0.050 in these cases, terms A and B are significance. On the contrary, the values increasing 0.100 indicate lack of significance in the model [42] Reducing the model, except for essential hierarchical elements, may improve its performance by diminishing the lack of significance. The 'Lack' of Fit F-value, which is 183.71, emphasizes the importance value of addressing the Lack of Fit. The presence of noise contributing to a Lack of Fit F-value of this magnitude is only 0.54%.A noteworthy Lack of Fit is undesirable, as our goal is to ensure a well-fitting model.

The Predicted R^2, standing at 0.5202, closely corresponds to Adjusted R^2 of 0.6778, with a difference of less than 0.2 adequate Precision assesses the ratio of 'signal to noise', favouring a ratio exceeding 4 [43, 20] with an impressive ratio of 11.005, this model exhibits a strong signal, making it well-suited for exploring and navigating the design space.

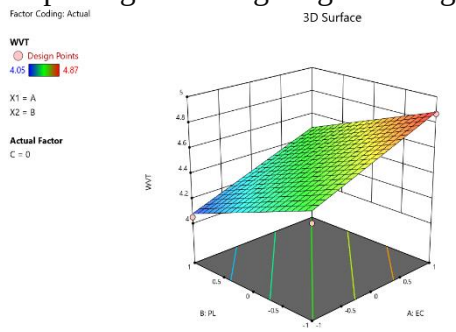

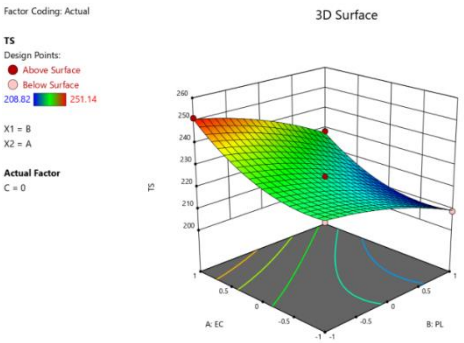

(a) **(b)**

Figure 4: 3D response surface plot a) showing influence of polymer concentration, plasticizer concentration and permeation enhancer concentration on Moisture content (b) indicating influence of polymer concentration, plasticizer concentration and permeation enhancer concentration on Tensile strength.

Model F-value, registering at 70.28, signifies the model's significance, with a mere 0.01% probability of such a huge F-value occurring due to 'noise'. Model are considered as significant when their P-values are lower than 0.050, and the terms A, B, AC, A^2, B^2 and C^2 all deemed remarkable. Increasing 0.1000 values indicates insignificance of model terms [44]. If numerous terms lack significance (excluding those essential for hierarchy), reducing the model may enhance its performance. The 'Lack of Fit' F-value, standing at 18.22, implies a 5.25% chance of such a large value occurring due to noise. A significant 'Lack of Fit'is undesirable, because the goal is ensure the model fits well. The relatively low probability, less than 10%, raises concerns about the model's adequacy [45].

The forecast R^2, documented at 0.8783, closely matches the Adjusted R^2 of 0.9780, showcasing a difference of less than 0.2. Adeq Precision, which evaluates the signal-to-noise ratio, favors a ratio surpassing 4. With a strong ratio of 27.385, this model exhibits a substantial signal. As a result, it is highly suitable for 'navigating the design space' [46].

The Model F-value, measuring at 14.64, signifies the significance of model, with only a 0.04% probability of such a substantial F-value arising from noise. P-values below 0.0500 indicate the importance of the model, and the term B stands out as noteworthy. Conversely, values exceeding 0.1000 suggest the lack of significance in model terms.[47,18] If there are numerous insignificant terms (excluding those essential for hierarchy), reducing the model could potentially enhance its effectiveness. The 'Lack of Fit' F-value, established at 0.63, indicates the 'Lack of Fit' is not significant compared to pure error. There is a 74.36% chance of a Lack of Fit F-value of this magnitude occurring due to 'noise'. A non-significant lack of fit is advantageous, as our goal is to achieve a well-fitting model.[48, 40]

Predicted R^2 value, positioned at 0.6260, closely corresponds to the Adjusted R^2 of 0.7469, with a disparity of under 0.2. 'Adeq Precision' assesses the signal-to-noise ratio, favouring a ratio surpassing 4. With a strong ratio of 10.238, this model demonstrates a substantial signal, making it well-suited for navigating the design space. [49]

The results of skin irritation studies are given in table 3 no dermatological changes were observed in any grouped animal using Diclofenac potassium drug. There was no skin responses of erythema, eachar or edema, were observed in rabbit skin.

Table 3: Skin irritation study of Diclofenac potassium at different time period in Rabbit

Formulations	**Erythema**	**Oedema**
Acute singled skin irritation study		
1hr. after removal of formulation	**0**	**0**
24hr. after removal of formulation	**0**	**0**
48hr. after removal of formulation	**0**	**0**
72hr. after removal of formulation	**0**	**0**
Acute repeated skin irritation study		

1hr. after removal of formulation	**0**	**0**
24hr. after removal of formulation	**0**	**0**
48hr. after removal of formulation	**0**	**0**
72hr. after removal of formulation	**0**	**0**

Discussion

All patches 'folding endurance values 'were considered to be good, indicates that patches formulated by Glycerine (plasticizer) were having 'optimum flexibility' and were not brittle. The weight of patches prepared by EU100 and PL were found in between 0.20-0.21 gm. All the patches showed uniformity in weight which indicative of efficiency of solvent casting process [50].

Drug was subjected to an FT-IR analysis and identifies the compounds. Diclofeanac was carefully put over the sample holder for scanning. FT-IR spectrum for a pure drug and drug-polymer was done. Drug-excipient interactions are essential for, among other things, release, and the medication from the 'formulation'. Here, the 'physical and chemical interactions' between the 'drug' and 'excipients' have been investigated using FT-IR techniques. Figure 1 depicts the infrared (IR) spectra of the mixture of DI-K with excipients of PU & AC formulation (A).[51] Infrared absorption spectroscopy (IR) of DI-K revealed to stretching vibration at 3549.14, 3387.88, and 831 cm^{-1} of OH, N-H and C-Cl respectively (Figure 1). The Infrared absorption spectroscopy (IR) of DI-K revealed sharp bands at 3439.66, 3377.68, and 882.90 cm^{-1}, which were caused by stretching of the vibration bands of OH, N-H, and C-Cl, respectively (Figure 1). The primary peaks in the IR spectra of 'drug and polymer' mixture did not change, as seen in the image, indicating that there were no physical interactions due to bond formation between the drug and polymer [52,53].

The 'tensile strength' of the 'patches' having EU100 and PL as found in between 210.50 gm/cm^2 to 253.31 gm/cm^2. It became known that with increase in concentration in hydrophilic polymers PL the 'tensile strength' of the 'formulation' decreases gradually. The water vapour transmissions of patches were found to between in case of EU100-PL 1.16059 $x10^{-4}$ to 1.91012 X 10^{-4}, which show the patches were permeable to water. It became known that that with the increase of' hydrophilic polymer' the WVRT was increased and F5 has shown the least water vapour transmission profile probably as a result of the lesser amount of hydrophilic polymer. The present moisture content of the patches prepared with different proportion of EU- PL were found to be in between and for the patches developed with 4.05 to 4.82%. From this result it was observed that increases the concentration of hydrophilic polymer of different formulations moisture content also increasing accordingly.[54] As F10 contain highest amount of EU100, 'moisture content' is low, which is reverse in case of F5. But little 'moisture content' in the patches helps the material to remain stable and not to become completely dry and brittle. The % 'moisture uptake' of the patches prepared with different proportion of EU100 and PL were found to be in between (Table 3) 2.64 to 6.92%. From this result it was observed that increases the concentration of hydrophilic polymer of moisture uptake also increased accordingly. As F5 contain highest amount of PL, moisture uptake is highest, which is reverse in case of F5.[55,56] Simultaneously low 'moisture uptake' protects the patches from 'microbial contamination' and

'bulkiness'. The thickness of the patches prepared by EU 100 and PL were found in between 102-114 micron. These types of thickness totally depend on casting solution and the using plasticizer, dibutyl phthalate. A low 'standard deviation' value in the patch thickness measurement confirms uniformity of the patches prepared by solvent evaporation technique.[57] The results of flatness study (Table 3) it was observed that none of the formulation had the knot same in the strip lengths before and after their cuts, thus indicating more than 99% flatness. [58] It indicates no constriction in the films and thus they could maintain a smooth surface when applied onto the skin leading to intimate contact and hence better drug permeation [22] JEOL, JSM-6360 scanning electron microscope was used for the surface morphologies study of films at 7 kv.[59.60] Before the study the patch pieces were gold-coated to render them electrically conductive[61]. There was no dermatological changes were observed in any grouped animal using Diclofenac potassium drug. There was no skin responses of erythema, eachar or oedema, were observed in rabbit skin.

Conclusion

The process outlined in this research paper for creating Diclofenac potassium transdermal films is straightforward. The physicochemical characteristics of each formulation, including thickness, weight variation, drug content, flatness, folding durability, 'moisture content and moisture uptake', all exhibited satisfactory performance. *In-vitro* release value revealed that types of polymers and their concentrations influenced the drug release from the patch formulation. Regarding 'in-vitro drug permeation' and 'skin irritation study' the impact of penetration enhancer concentration was investigated. These studies indicated that drug permeability increased when the penetration enhancer concentration reached an optimal level. This investigation suggests that applying Diclofenac potassium topically to the affected area can address issues associated with its oral delivery, such as dissolving rate, limited absorption, and gastrointestinal side effects.

References:

1. Ng LC, Gupta M. Transdermal drug delivery systems in diabetes management: A review. Asian journal of pharmaceutical sciences. 2020 Jan 1;15(1):13-25. doi: 10.1016/j.ajps.2019.04.006
2. Han W, Liu F, Li Y, Liu G, Li H, Xu Y, Sun S. Advances in Natural Polymer-Based Transdermal Drug Delivery Systems for Tumor Therapy. Small. 2023 Aug;19(35):2301670. doi: 10.1002/smll.202301670
3. Franco P, De Marco I. The Use of Poly (N-vinyl pyrrolidone) in the Delivery of Drugs: A Review. Polymers. 2020 May 13;12(5):1114. doi: 10.3390/polym12051114
4. Mangang KN, Thakran P, Halder J, Yadav KS, Ghosh G, Pradhan D, et al. PVP-microneedle array for drug delivery: Mechanical insight, biodegradation, and recent advances. Journal of Biomaterials Science, Polymer Edition. 2023 May 3;34(7):986-1017. doi: 10.1080/09205063.2022.2155778..
5. Qiang N, Liu Z, Lu M, Yang Y, Liao F, Feng Y,et al. Preparation and Properties of Polyvinylpyrrolidone/Sodium Carboxymethyl Cellulose Soluble Microneedles. Materials. 2023 Apr 27;16(9):3417. doi: 10.3390/ma16093417
6. Gupta V, Singh S, Srivarstava M, Ahmad H, Pachauri SD, Khandelwal K, et al, CDRI communication no: 8635. Effect of polydimethylsiloxane and ethylcellulose on in vitro

permeation of centchroman from its transdermal patches. Drug delivery. 2016 Jan 2;23(1):113-22. doi: 10.3109/10717544.2014.905882

7. Panigrahi L, Pattnaik S, Ghosal SK. The effect of pH and organic ester penetration enhancers on skin permeation kinetics of terbutaline sulfate from pseudolatex-type transdermal delivery systems through mouse and human cadaver skins. Aaps Pharmscitech. 2005 Jun;6:E167-73. doi: 10.1208/pt060225
8. Massias T, de Paiva Lacerda S, de Azevedo JR, Letourneau JJ, Bolzinger MA, Espitalier F. Supercritical carbon dioxide solubility measurement and modelling for effective size reduction of nifedipine particles for transdermal application. International Journal of Pharmaceutics. 2023 Jan 5;630:122425. doi: 10.1016/j.ijpharm.2022.122425,
9. Hutton AR, Ubah O, Barelle C, Donnelly RF. Enhancing the transdermal delivery of 'next generation'variable new antigen receptors using microarray patch technology: a proof-of-concept study. Journal of Pharmaceutical Sciences. 2022 Dec 1;111(12):3362-76. doi: 10.1016/j.xphs.2022.08.027.
10. Akhlaq M, Arshad MS, Mudassir AM, Hussain A, Kucuk I, Haj-Ahmad R, et al. Formulation and evaluation of anti-rheumatic dexibuprofen transdermal patches: a quality-by-design approach. Journal of drug targeting. 2016 Aug 8;24(7):603-12. doi: 10.3109/1061186X.2015.1116538
11. Suksaeree J, Thuengernthong A, Pongpichayasiri K, Maneewattanapinyo P, Settharaksa S, Pichayakorn W. Formulation and evaluation of matrix type transdermal patch containing silver nanoparticles. Journal of Polymers and the Environment. 2018 Dec;26:4369-75. doi: 10.1007/s10924-018-1305-5
12. Rhee YS, Nguyen T, Park ES, Chi SC. Formulation and biopharmaceutical evaluation of a transdermal patch containing aceclofenac. Archives of pharmacal research. 2013 May;36:602-7. doi: 10.1007/s12272-013-0073-y
13. Murthy SN, Rani S, Hiremath R. Formulation and evaluation of controlled-release transdermal patches of theophylline–salbutamol sulfate. Drug development and industrial pharmacy. 2001 Jan 1;27(10):1057-62. doi: 10.1081/ddc-100108368
14. Rai A, Sharma R, Dewangan HK. Formulation and evaluation of polymeric transdermal patch of meloxicam. Materials Today: Proceedings. 2022 Jan 1;68:803-8. doi: 10.1016/j.mat¬pr.2022.06.156.
15. Costa RR, Neto AI, Calgeris I, Correia CR, Pinho AC, Fonseca J, Öner ET, Mano JF. Adhesive nanostructured multilayer films using a bacterial exopolysaccharide for biomedical applications. Journal of Materials Chemistry B. 2013;1(18):2367-74.
16. Sanap GS, Dama GY, Hande AS, Karpe SP, Nalawade SV, Kakade RS, et al. Preparation of transdermal monolithic systems of indapamide by solvent casting method and the use of vegetable oils as permeation enhancer G. International Journal of Green Pharmacy (IJGP). 2008;2(2).
17. Al Hanbali OA, Khan HM, Sarfraz M, Arafat M, Ijaz S, Hameed A. Transdermal patches: Design and current approaches to painless drug delivery. Acta Pharmaceutica. 2019 Jun 30;69(2):197-215. doi: 10.2478/acph-2019-0016.
18. Carter P, Narasimhan B, Wang Q. Biocompatible nanoparticles and vesicular systems in transdermal drug delivery for various skin diseases. International journal of pharmaceutics. 2019 Jan 30;555:49-62. doi: 10.1016/j.ijpharm.2018.11.032

19. Hashmat D, Shoaib MH, Ali FR, Siddiqui F. Lornoxicam controlled release transdermal gel patch: Design, characterization and optimization using co-solvents as penetration enhancers. Plos one. 2020 Feb 27;15(2):e0228908. doi: 10.1371/journal.pone.0228908.
20. Leone M, Mönkäre J, Bouwstra JA, Kersten G. Dissolving microneedle patches for dermal vaccination. Pharmaceutical research. 2017 Nov;34:2223-40. doi: 10.1007/s11095-017-2223-2. Epub 2017 Jul 17.
21. Su Y, Lu W, Fu X, Xu Y, Ye L, Yang J, Huang H,et al. Formulation and pharmacokinetic evaluation of a drug-in-adhesive patch for transdermal delivery of koumine. AAPS PharmSciTech. 2020 Nov;21:1-1. doi: 10.1208/s12249-020-01793-y
22. Ravula R, Herwadkar AK, Abla MJ, Little J, Banga AK. Formulation optimization of a drug in adhesive transdermal analgesic patch. Drug development and industrial pharmacy. 2016 Jun 2;42(6):862-70. doi: 10.3109/03639045.2015.1071832. Epub 2015 Jul 31
23. Schurad B, Koch C, Schug B, Morte A, Vaqué A, De la Torre R, Iniesta M. Comparative bioavailability study of a novel multi-day patch formulation of rivastigmine (twice weekly) with Exelon® transdermal patch (Daily)-A randomized clinical trial. Current Alzheimer Research. 2022 Nov 11;19(7):541. doi: 10.2174/1567205019666220823105059
24. Morte A, Vaqué A, Iniesta M, Schug B, Koch C, De la Torre R, Schurad B. Bioavailability Study of a Transdermal Patch Formulation of Rivastigmine Compared with Exelon in Healthy Subjects. European Journal of Drug Metabolism and Pharmacokinetics. 2022 Jul;47(4):567-78. doi: 10.1007/s13318-022-00778-5
25. González-Rojano E, Marcotegui J, Morales-Alcelay S, Álvarez C, Gordon J, Abad-Santos F, et al A. Sex-by-formulation interaction in bioequivalence trials with transdermal patches. European Journal of Clinical Pharmacology. 2019 Jun 1;75:801-8. doi: 10.1007/s00228-019-02632-1.
26. Afanasjeva J, Gabay M, Poznanski T, Kerns S. Transdermal Patch Administration and Magnetic Resonance Imaging (MRI)—2020. Hospital Pharmacy. 2022 Feb;57(1):117-20. doi: 10.1177/0018578720987138.
27. Rhee YS, Nguyen T, Park ES, Chi SC. Formulation and biopharmaceutical evaluation of a transdermal patch containing aceclofenac. Archives of pharmacal research. 2013 May;36:602-7. doi: 10.1007/s12272-013-0073-y
28. Cawello W, Wolff HM, Meuling WJ, Horstmann R, Braun M. Transdermal administration of radiolabelled [14 C] rotigotine by a patch formulation: a mass balance trial. Clinical pharmacokinetics. 2007 Oct;46:851-7. doi: 10.2165/00003088-200746100-00003.
29. Saleem MN, Idris M. Formulation design and development of a unani transdermal patch for antiemetic therapy and its pharmaceutical evaluation. Scientifica. 2016 Jun 15;2016. :1-5 doi: 10.1155/2016/7602347
30. Hai NT, Kim J, Park ES, Chi SC. Formulation and biopharmaceutical evaluation of transdermal patch containing benztropine. International journal of pharmaceutics. 2008 Jun 5;357(1-2):55-60. doi: 10.1016/j.ijpharm.2008.01.024.
31. Patel RP, Gaiakwad DR, Patel NA. Formulation, optimization, and evaluation of a transdermal patch of heparin sodium. Drug discoveries & therapeutics. 2014 Aug 31;8(4):185-93. doi: 10.5582/ddt.2014.01030

32. Ravula R, Herwadkar AK, Abla MJ, Little J, Banga AK. Formulation optimization of a drug in adhesive transdermal analgesic patch. Drug development and industrial pharmacy. 2016 Jun 2;42(6):862-70. doi: 10.3109/03639045.2015.1071832
33. Davis MP, Pasternak G, Behm B. Treating chronic pain: an overview of clinical studies centered on the buprenorphine option. Drugs. 2018 Aug;78:1211-28. doi: 10.1007/s40265-018-0953-z.
34. Ameen D, Michniak-Kohn B. Development and in vitro evaluation of pressure sensitive adhesive patch for the transdermal delivery of galantamine: Effect of penetration enhancers and crystallization inhibition. European Journal of Pharmaceutics and Biopharmaceutics. 2019 Jun 1;139:262-71. . doi: 10.1016/j.ejpb.2019.04.008.
35. Hadgraft J, Lane ME. Drug crystallization–implications for topical and transdermal delivery. Expert opinion on drug delivery. 2016 Jun 2;13(6):817-30. doi:10.1517/17425247.2016.1140146.
36. Wang J, Li Z, Sun F, Tang S, Zhang S, Lv P,et al. Evaluation of dermal irritation and skin sensitization due to vitacoxib. Toxicology Reports. 2017 Jan 1;4:287-90. doi.org/10.1016/j.toxrep.2017.06.003
37. Lobo S, Sachdeva S, Goswami T. Role of pressure-sensitive adhesives in transdermal drug delivery systems. Therapeutic delivery. 2016 Jan;7(1):33-48. doi: 10.4155/tde.15.87
38. Kim SH, Jeong JY, Park HJ, Moon BM, Park YR, Lee OJ, et al. Application of a collagen patch derived from duck feet in acute tympanic membrane perforation. Tissue Engineering and Regenerative Medicine. 2017 Jun;14:233-41. doi:10.1007/s13770-017-0039-0.
39. Akram MR, Ahmad M, Abrar A, Sarfraz RM, Mahmood A. Formulation design and development of matrix diffusion controlled transdermal drug delivery of glimepiride. Drug design, development and therapy. 2018 Feb 21:349-64. doi: 10.2147/DDDT.S147082
40. Park CW, Son DD, Kim JY, Oh TO, Ha JM, Rhee YS, et al. Investigation of formulation factors affecting in vitro and in vivo characteristics of a galantamine transdermal system. International journal of pharmaceutics. 2012 Oct 15;436(1-2):32-40. doi: 10.1016/j.ijpharm.2012.06.057
41. Jain P, Banga AK. Inhibition of crystallization in drug-in-adhesive-type transdermal patches. International journal of pharmaceutics. 2010 Jul 15;394(1-2):68-74. Available from: https://linkinghub.elsevier.com/retrieve/pii/S0378517310003145.
42. Furuishi T, Io T, Fukami T, Suzuki T, Tomono K. Formulation and in vitro evaluation of pentazocine transdermal delivery system. Biological and Pharmaceutical Bulletin. 2008 Jul 1;31(7):1439-43. doi: 10.1248/bpb.31.1439.
43. Sun Y, Fang L, Zhu M, Li W, Meng P, Li L, et al. A drug-in-adhesive transdermal patch for S-amlodipine free base: in vitro and in vivo characterization. International Journal of Pharmaceutics. 2009 Dec 1;382(1-2):165-71. doi: 10.1016/j.ijpharm.2009.08.031
44. Soler LI, Boix A, Lauroba J, Colom H, Domenech J. Transdermal delivery of alprazolam from a monolithic patch: formulation based on in vitro characterization. Drug Development and Industrial Pharmacy. 2012 Oct 1;38(10):1171-8. doi: 10.3109/03639045.2011.643893

45. Pu T, Li X, Sun Y, Ding X, Pan Y, Wang Q. Development of a prolonged-release pramipexole transdermal patch: in vitro and in vivo evaluation. AAPS PharmSciTech. 2017 Apr;18:738-48. doi: 10.1208/s12249-016-0555-6.
46. Subedi RK, Ryoo JP, Moon C, Choi HK. Influence of formulation variables in transdermal drug delivery system containing zolmitriptan. International journal of pharmaceutics. 2011 Oct 31;419(1-2):209-14. doi: 10.1016/j.ijpharm.2011.08.002
47. Sun L, Cun D, Yuan B, Cui H, Xi H, Mu L, Chen Y, Liu C, Wang Z, Fang L. Formulation and in vitro/in vivo correlation of a drug-in-adhesive transdermal patch containing azasetron. Journal of pharmaceutical sciences. 2012 Dec 1;101(12):4540-8. . doi: 10.1002/jps.23317
48. Liu C, Qu X, Song L, Shang R, Wan X, Fang L. Investigation on the effect of deep eutectic formation on drug-polymer miscibility and skin permeability of rotigotine drug-in-adhesive patch. International Journal of Pharmaceutics. 2020 Jan 25;574:118852. doi: 10.1016/j.ijpharm.2019.118852
49. Chen Y, Quan P, Liu X, Guo W, Song W, Cun D, et al. Enhancement of skin permeation of flurbiprofen via its transdermal patches using isopulegol decanoate (ISO-C10) as an absorption enhancer: pharmacokinetic and pharmacodynamic evaluation. Journal of Pharmacy and Pharmacology. 2015 Sep;67(9):1232-9. doi: 10.1111/jphp.12428.
50. Heard CM, Johnson S, Moss G, Thomas CP. In vitro transdermal delivery of caffeine, theobromine, theophylline and catechin from extract of Guarana, Paullinia Cupana. International Journal of Pharmaceutics. 2006 Jul 6;317(1):26-31. doi: 10.1016/j.ijpharm.2006.02.042
51. K Das M, Yelhounganba Khuman L. Ex vivo permeation kinetics of zidovudine from pseudolatex acrylic film across pig ear epidermis. Current Drug Delivery. 2012 Sep 1;9(5):468-76. doi: 10.2174/156720112802650671
52. Mundada AS, Avari JG. Novel biomaterial for transdermal application: in vitro and in vivo characterization. Drug Delivery. 2011 Aug 1;18(6):424-31. doi: 10.3109/10717544.2011.577107
53. Hadgraft J, Lane ME. Drug crystallization–implications for topical and transdermal delivery. Expert opinion on drug delivery. 2016 Jun 2;13(6):817-30. doi:10.1517/17425247.2016.1140146
54. Jiang Q, Wang J, Ma P, Liu C, Sun M, Sun Y, He Z. Ion-pair formation combined with a penetration enhancer as a dual strategy to improve the transdermal delivery of meloxicam. Drug delivery and translational research. 2018 Feb;8:64-72. doi: 10.1007/s13346-017-0434-z.
55. Vora D, Banga AK. Development and evaluation of a drug-in-adhesive transdermal delivery system for delivery of olanzapine. Expert Opinion on Drug Delivery. 2022 Nov 2;19(11):1539-48. doi: 10.1080/17425247.2022.2135700.
56. Hashmat D, Shoaib MH, Ali FR, Siddiqui F. Lornoxicam controlled release transdermal gel patch: Design, characterization and optimization using co-solvents as penetration enhancers. Plos one. 2020 Feb 27;15(2):e0228908. doi: 10.1371/journal.pone.0228908.
57. Yang Z, Teng Y, Wang H, Hou H. Enhancement of skin permeation of bufalin by limonene via reservoir type transdermal patch: formulation design and biopharmaceutical evaluation. International journal of pharmaceutics. 2013 Apr 15;447(1-2):231-40. doi: 10.1016/j.ijpharm.2013.02.048.

58. Ahmed TA, Khalid M. Development of alginate-reinforced chitosan nanoparticles utilizing W/O nanoemulsification/internal crosslinking technique for transdermal delivery of rabeprazole. Life sciences. 2014 Aug 6;110(1):35-43. doi: 10.1016/j.lfs.2014.06.019
59. Aggarwal G, Dhawan S, L HariKumar S. Natural oils as skin permeation enhancers for transdermal delivery of olanzapine: in vitro and in vivo evaluation. Current Drug Delivery. 2012 Mar 1;9(2):172-81. doi: 10.2174/156720112800234567
60. Yang D, Liu C, Piao H, Quan P, Fang L. Enhanced drug loading in the drug-in-adhesive transdermal patch utilizing a drug–ionic liquid strategy: insight into the role of ionic hydrogen bonding. Molecular Pharmaceutics. 2021 Jan 28;18(3):1157-66. doi: 10.1021/acs.molpharmaceut.0c01054
61. Woo FY, Basri M, Fard Masoumi HR, Ahmad MB, Ismail M. Formulation optimization of galantamine hydrobromide loaded gel drug reservoirs in transdermal patch for Alzheimer's disease. International Journal of Nanomedicine. 2015 Jun 5:3879-86. doi: 10.2147/IJN.S80253